

Interfacing Soft and Hard Materials with Triple-Shape-Memory and Self-Healing Functions

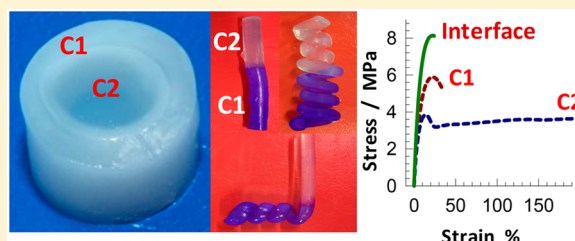
Aslihan Argun,[†] Umit Gulyuz,^{†,‡} and Oguz Okay^{*,†}

[†]Department of Chemistry, Istanbul Technical University, 34469 Maslak, Istanbul, Turkey

[‡]Department of Chemistry and Chemical Processing Technologies, Kırklareli University, 39750 Luleburgaz, Kırklareli, Turkey

Supporting Information

ABSTRACT: Many natural materials such as intervertebral disk (IVD) are composed of regions with large mismatches in the mechanical properties, yet these regions are integrated through an extremely tough interface. To mimic the mechanical heterogeneity inherent in biological systems, we present here mechanically strong hydrogels consisting of hard and soft components joined together through a strong interface. Stratification of monomer solutions having different densities was used to create two layers of monomer solutions with an interlayer region of a few millimeters in thickness, at which the solutions mix completely. UV-initiated bulk copolymerization of stratified solutions of hydrophilic and hydrophobic monomers leads to the formation of supramolecular, semicrystalline hard/soft hydrogel hybrids with tunable mechanical and thermal properties. By adjusting the comonomer composition in the stratified layers, we were able to create gel/gel interfaces in hybrids that are stronger than their gel components so that they never rupture at the interface region. The hybrids exhibit a high modulus (0.46–74 MPa), tensile strength (0.19–3.9 MPa), and sustain 24–30 MPa stresses at 78–83% compressions, which are comparable to the natural IVD. They also exhibit thermally induced self-healing behavior as well as pseudo triple-shape-memory effect arising from different melting temperatures of crystalline domains belonging to the gel components of hybrids.



INTRODUCTION

Hydrogels are soft and intelligent materials with some similarities to biological systems.^{1–3} In recent years, significant progress has been achieved in the preparation of mechanically strong and tough hydrogels by creating an effective energy dissipation in the gel network.⁴ High strength hydrogels reported so far are isotropic materials exhibiting identical chemical compositions and mechanical properties in all directions and locations. In contrast, many biological systems are combinations of hard and soft materials with extremely tough interfaces between their components. For instance, connective tissues such as tendon are joined to bone in a specialized interface known as the enthesis.^{5,6} Despite the large mismatches in the mechanical properties of tendon and bone, e.g., their tensile moduli are ~0.45 and 20 GPa, respectively, the enthesis can bear loads equivalent to multiples of the body weight.^{5,6} Rather than enthesis failure, bone avulsion or tendon rupture tends to occur under overloading. Another example is the intervertebral disk (IVD) locating between vertebral bodies and providing flexibility, load transfer, and energy dissipation to the spine. IVD consists of a highly swollen, gelatinous soft core (nucleus pulposus, NP), surrounded by a thinner less swollen, mechanically strong outer layer (annulus fibrosus, AF), yet the two regions are integrated into a single fused material.^{7–9} As a result of this structure, IVD sustains millions of continuous loading and unloading cycles without damage.

Interfacing soft materials with hard ones is an area of research being addressed in the past few years. Hu et al.

prepared “modulated hydrogels” by swelling the first gel component in excess of a second monomer solution followed by cross-linking copolymerization.¹⁰ However, because the second monomer is completely mixed with the first gel, an interpenetrated network hydrogel component could be produced by this technique. Raghavan and co-workers were the first to realize hydrogels comprising of two dissimilar gel components, which will be called thereafter hybrid hydrogels.^{11,12} They were prepared by bringing two high-viscosity monomer solutions into contact and then polymerizing the system. The key of this approach is the limited diffusion of the monomer solutions at the gel/gel interface providing formation of smooth, robust interfaces between dissimilar gel zones and preserving the properties of each individual gel component.¹¹ “Gluing” together separate gel samples is another mean to create hybrid hydrogels with two or more distinct regions.^{13–15} Leibler et al. used nanoparticles as a binding agent to glue dry or swollen hydrogels together.¹³ Yong et al. extended this approach to the preparation of multilayered hydrogel sheets by photoinitiated polymerization.^{16,17} They used atom transfer radical polymerization to effectively add one layer on top of the other through successive polymerization reactions resulting in chemical cross-links binding polymer chains between successive layers. Another method to join dissimilar materials utilizes rapid

Received: February 1, 2018

Revised: March 14, 2018

Published: March 19, 2018

Scheme 1. Structure of the Monomer Units (Upper Panel) and Optical Images of C1/C2 and C1/C3 Hybrid Hydrogels (Bottom Panel)

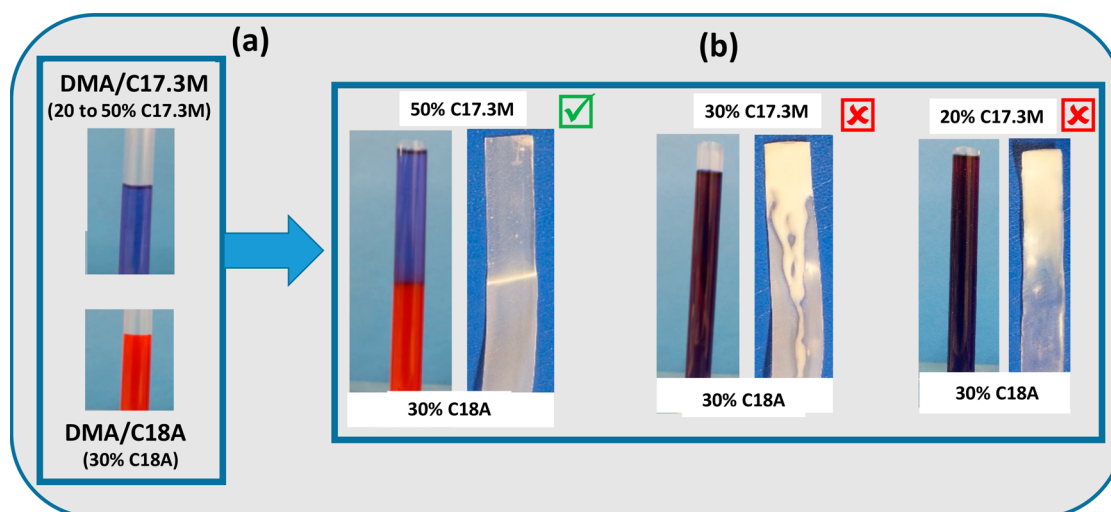
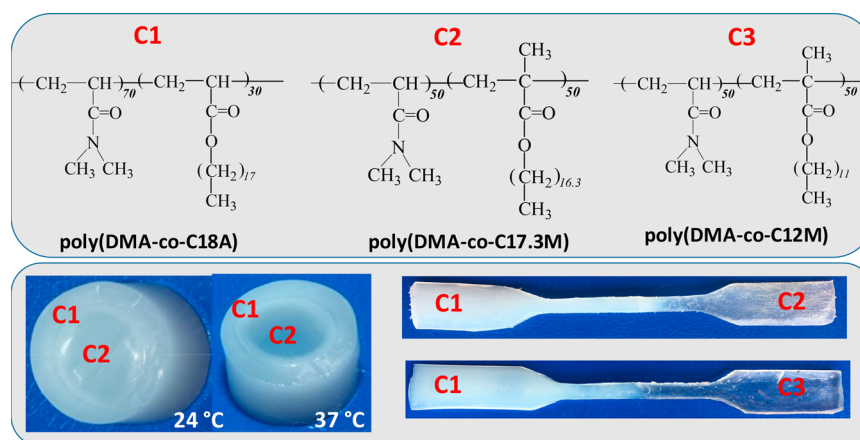


Figure 1. (a) Images of DMA/C17.3M and DMA/C18A monomer mixtures colored with blue and red, respectively. (b) Images of the monomer mixtures and resulting hybrid hydrogels after addition of DMA/C17.3M at various compositions on top of DMA/C18A at a molar ratio of 70/30.

adhesion between polyethylene glycol hydrogels swollen in water and organogels swollen in anisole, yielding macroscopic organo/hydrogel hybrids.¹⁸ Acylhydrazone dynamic bonds formed by condensation of the aldehyde and acylhydrazone groups between the macroscopic gels acted as “gluing” agents. Although this method allows reversible cross-links and hence enables self-healing function in the hybrid, it was applicable to a limited number of monomers.¹⁸ Moreover, the tensile strengths of hybrids and their components are below 0.1 MPa. Yuk et al. recently reported a strategy to design tough transparent and conductive bonding of hydrogels to nonporous solid surfaces.¹⁹ The strategy was to anchor the network chains of the hydrogels covalently to the surfaces which was achieved by their silanation. Because hybrid hydrogels have important potential applications as biomaterials and in tissue engineering, they should exhibit a high mechanical strength, modulus, and toughness. Previous studies summarized above reveal that they are not suitable for load-bearing applications. Considering the Young’s moduli of AF and NP components of human IVD, which are 22–28 and 3–8 MPa in the linear regime, respectively,^{7,20–22} the replication of IVD using synthetic hybrid hydrogels requires a modulus in the range of MPa.

Here we present a design strategy and preparation methods of mechanically strong hybrid hydrogels consisting of hard and soft components with a strong interface, thus mimicking the mechanical heterogeneity inherent in biological systems. We use stratification of monomer solutions of different densities followed by polymerization of stratified solutions. The inspiration of this work came from the water stream in the Istanbul strait (Bosphorus), a typical narrow sea strait connecting two seas, where more saline Mediterranean water flows at the bottom layer while the less saline Black Sea water flows at the top layer in the reverse direction. Similarly, by adjusting the densities of two monomer solutions, we were able to create two layers of monomer solutions with an interface at which the solutions mix completely. The challenge of this work was to find a mixed solution composition at the interface forming a stronger gel than the individual gel components.

Hydrophobic interactions were used to prepare supramolecular hybrid hydrogels with tunable mechanical and thermal properties.²³ Recent work shows that such interactions create semicrystalline hydrogels with extraordinary mechanical properties together with shape-memory and self-healing functions.^{24–26} Hybrid hydrogels were prepared by a simple UV-initiated bulk copolymerization of stratified solutions of

hydrophilic and hydrophobic monomers and subsequent swelling of the resulting copolymers in water. *N,N*-Dimethylacrylamide (DMA) was selected as the hydrophilic monomer due to the hydrophilicity, biocompatibility, and associative properties of the resulting polymer.^{27,28} *n*-Octadecyl acrylate (C18A), stearyl methacrylate (C17.3M), and lauryl methacrylate (C12M) were selected as the hydrophobic monomers with long alkyl side chains able to form crystalline domains and/or hydrophobic associations in hydrogels (Scheme 1).^{24,29} As will be seen below, by adjusting the composition of DMA/C18A, DMA/C17.3M, and DMA/C12M monomer mixtures in stratified solutions, we were able to create mechanically strong hybrid hydrogels that never rupture at their gel/gel interface. The hybrids exhibit a high modulus (0.46–74 MPa) and tensile strength (0.19–3.9 MPa) and sustain 24–30 MPa stresses at 78–83% compressions, which are comparable to the natural IVD.^{7,20–22} They also exhibit thermally induced self-healing behavior and pseudo triple-shape-memory effect arising from different melting temperatures of crystalline domains belonging to the gel components of hybrids.

EXPERIMENTAL PART

Materials. *N,N*-Dimethylacrylamide (DMA), stearyl methacrylate (C17.3M), a mixture of 65% *n*-octadecyl methacrylate and 35% *n*-hexadecyl methacrylate, *n*-octadecyl acrylate (C18A), lauryl methacrylate (C12M), and Irgacure 2959 were all purchased from Sigma-Aldrich (St. Louis, MO) and used without purification.

Stratification of the Monomer Solutions. The preparation of hybrid hydrogels in rectangular shape with two distinct gel zones is based on the density difference of the monomer mixtures, measured using a calibrated glass pycnometer at 25 °C. The solution with a low density floats on top of another solution of higher density whereas the interface between layers acts as a barrier to prevent monomers from diffusion between layers. For instance, Figure 1a shows two plastic tubes containing DMA/C18A and DMA/C17.3M monomer mixtures, colored with red and blue, respectively. The molar ratio of DMA/C18A was fixed at 70/30, at which it has a density of 0.894 g mL⁻¹. The density of DMA/C17.3M increases from 0.881 to 0.912 g mL⁻¹ as its C17.3M content is decreased from 50 to 20 mol %. When the blue DMA/C17.3M solution is dropwise added on top of the red DMA/C18A (Figure 1b), a distinct interface appears at 50 mol % C17.3M content because of its lowest density among other solutions. Inversely, when red DMA/C18A solution is added on top of blue DMA/C17.3M solutions, solution containing 20 mol % C17.3M is the best because of its highest density (Figure S1). Several tests showed that the following comonomer compositions lead to the formation of hybrid hydrogels with a distinct interface that is stronger than the gel components (Figure S2): (i) DMA/C18A monomer mixture at a molar ratio of 70/30, denoted as M1 solution; (ii) DMA/C17.3M and DMA/C12M monomer mixtures at equal molar ratios, denoted as M2 and M3 solutions, respectively.

Moreover, the viscosity of M1 solution during polymerization increased much more rapidly as compared to that of the other solutions, and M1 turned to a gel after 10 min, while both M2 and M3 formed gels after more than 1 h (Figure S3). This difference in the gelation times between the layered solutions also prevented their mixing during the course of polymerization.

Preparation of Hybrid Hydrogels. Hybrid hydrogels were prepared by UV-initiated bulk copolymerization of the monomer mixtures using 0.1 wt % Irgacure 2959 photoinitiator (with respect to the monomers). Plastic molds of 80 × 14 × 1.5 mm dimension were used to prepare flat rectangular shaped hybrids. M1, M2, and M3 monomer mixtures (each 10 g) were first heated to 45 °C and then mixed with 5 mg of Irgacure initiator. After stirring the solutions for 5 min followed by cooling to 24 ± 3 °C, half of the mold was filled with M1 monomer mixture using a syringe, and then the second mixture (M2 or M3) was dropwise added on top of the first mixture, as

schematically illustrated in Figure 2a. The polymerization reactions were then conducted at 24 ± 3 °C for 24 h under UV light at 360 nm.

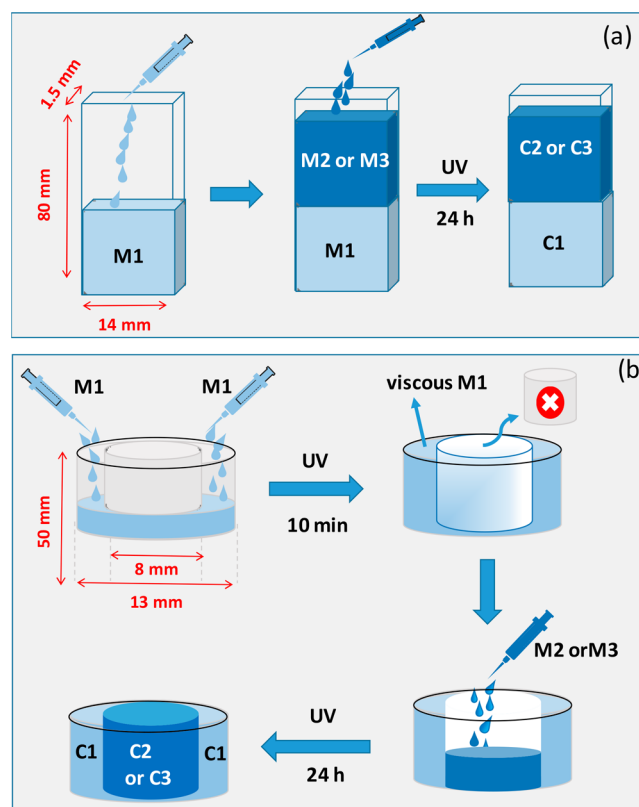


Figure 2. Preparation procedure of hybrid hydrogels in flat rectangular (a) and cylindrical shapes (b).

To compare the properties of hybrids with their gel components, bulk polymerizations of M1, M2, and M3 monomer mixtures were also carried out separately using 0.1 wt % Irgacure 2959, as described above. The reactions were carried out in syringes of internal diameters 13 and 25 mm as well as in rectangular plastic molds (80 × 14 × 1.5 mm). The stratification approach used in the preparation of hybrid hydrogels necessarily results in an interface where both monomer solutions completely mix so that the comonomer composition at the interface is the average of the two solutions. To mimic the properties of the interface region, mixture gels were prepared by mixing M1 with M2 and M1 with M3 before the onset of polymerization. The polymerization was then conducted as described above.

To design a hybrid material similar to the IVD, namely a material composed of a central soft core surrounded circumferentially by a hard gel, hybrid hydrogels were prepared using the limited diffusion approach described by Raghavan et al.¹¹ The mold used for this purpose consists of a plastic cylinder of 13 mm diameter and a Teflon pipe of 8 mm diameter located in the center of the cylinder (Figure 2b). M1 monomer mixture containing the initiator was first transferred outside of the Teflon pipe and then polymerized under UV light for 10 min to obtain a partially formed hydrogel. Teflon pipe was then removed from the mold, and the empty core was filled with M2 or M3 mixtures, each containing the initiator. The polymerization reactions were conducted at 24 ± 3 °C for 24 h under UV light at 360 nm.

Swelling and Gel Fraction Measurements. The copolymer samples thus obtained were immersed in excess of water at 70 and 23 ± 2 °C for the first and following days, respectively, for a duration of at least 10 days by replacing water every day to extract any soluble species. After equilibrium swelling, the amount of water in the gel samples was calculated as $H_2O\% = 10^2 \times (m - m_0)/m$, where m_0 and m are the initial and swollen mass of the gel samples. Then, the gel samples were freeze-dried, and the gel fraction W_g , that is, the

Table 1. Composition, Water Content, and Thermal and Tensile Mechanical Properties of the Gel Components, Mixture Gels, and Hybrids^a

code	composition (mol %)			H ₂ O (%)	T _m (°C)	T _{cry} (°C)	f _{cry} (%)	E (MPa)	ε _f (%)	σ _f (MPa)
	DMA	C18A	C17.3M							
C1/C2								74 (9)	113 (35)	3.9 (0.2)
C1/C3								0.46 (0.08)	457 (73)	0.19 (0.02)
C1	70	30		27	48	41	12	54 (4)	79 (3)	4.8 (0.6)
C2	50		50	10	35	23	12	88 (9)	287 (35)	4.0 (0.2)
C3	50			50	20		0	0.15 (0.02)	1140 (70)	0.13 (0.02)
C1 + C2	60	15	25	18	46	36	16	92 (2)	14 (3)	8.2 (0.9)
C1 + C3	60	15		25	15		0	0.49 (0.03)	1127 (160)	0.65 (0.13)

^aCompressive mechanical properties are given in Table S1.

conversion of monomers to the water-insoluble polymer, was calculated from the masses of dry polymer network and from the comonomer feed.

Rheological Experiments. Cylindrical gel samples of 12 and 25 mm in diameters and about 1 mm in thickness were used for the rheological tests. The measurements were carried out between the parallel plates of the rheometer (Gemini 150 Rheometer system, Bohlin Instruments) equipped with a Peltier device for temperature control. The upper plate (diameter 20 mm) was set at a distance of 1000–1250 μm, depending on the swelling degree of the hydrogels. During all rheological measurements, a solvent trap was used to minimize evaporation. Further, the outside of the upper plate was covered with a thin layer of low-viscosity silicone oil to prevent evaporation of solvent. A frequency ω of 6.3 rad s⁻¹ and a deformation amplitude $\gamma_0 = 0.001$ (0.1%) were selected to ensure that the oscillatory deformation is within the linear viscoelastic region. Thermal behavior of the gels was investigated by first keeping the samples at 80 °C for complete melting of crystalline domains and then, cooling down to 5 °C, after keeping for 10 min at 5 °C, heating back to 80 °C. The cooling/heating steps were carried out at a fixed rate of 1 °C min⁻¹. The changes in the dynamic moduli of gels were monitored during the course of the cycle as a function of temperature. The gel samples were also subjected to frequency-sweep tests at $\gamma_0 = 0.001$ over the frequency range 0.06–180 rad s⁻¹.

DSC Measurements. DSC measurements were conducted on a PerkinElmer Diamond DSC under a nitrogen atmosphere. The gel samples sealed in aluminum pans were scanned between 5 and 80 °C with a heating and cooling rate of 5 °C min⁻¹. From the DSC curves, enthalpy changes during melting, ΔH_m , were calculated from the peak areas. The degree of crystallinity, f_{cry} , that is, the fraction of polymer units in crystalline domains, was estimated by $f_{cry} = x_{HM}\Delta H_m / \Delta H_m^o$, where x_{HM} is the mole fraction of the hydrophobic monomer in the comonomer feed and ΔH_m^o is the melting enthalpy of crystalline C17.3M or C18A units. ΔH_m^o was taken as 71.2 kJ mol⁻¹ from previous works on the melting behavior of long *n*-alkyl chains exhibiting a hexagonal crystal structure.^{30–33}

Mechanical Tests. Uniaxial compression and elongation measurements were performed on swollen hydrogel samples on Zwick Roell and Devotrans test machines with 500 N and 10 kN load cells. All the tests were conducted at 24 ± 1 and 37 ± 1 °C. Load and displacement data were collected during the experiments. The Young's modulus E was calculated from the slope of stress–strain curves between 5 and 15% and 1–3% deformations for compression and elongation tests, respectively. For uniaxial compression measurements, cylindrical hydrogel samples of 6 ± 1 or 13 ± 1 mm in diameter and 7 ± 1 mm in length were compressed at a strain rate of 3.8 × 10⁻² s⁻¹. Before the test, an initial compressive contact to 0.01 ± 0.002 N was applied to ensure a complete contact between the gel and the plates. The stress was presented by its nominal σ_{nom} or true values σ_{true} (= $\lambda\sigma_{nom}$), which are the forces per cross-sectional area of the undeformed and deformed gel specimen respectively, while the compressive strain is given by λ , the deformation ratio (deformed length/initial length). The strain is also given by ϵ , the change in the sample length relative to its initial length; i.e., $\epsilon = 1 - \lambda$ or $\epsilon = \lambda - 1$ for compression and

elongation, respectively. Because the $\sigma_{true}-\lambda$ plots pass through maxima before a macroscopic fracture of the gel samples, the nominal fracture stress σ_f and the compression ratio ϵ_f at failure were calculated from the maxima in $\sigma_{true}-\lambda$ plots (Figure S4).³⁴ Uniaxial elongation measurements were performed on dumbbell-shaped hydrogel samples with the standard ISO-37 type 2 (ISO 527-2) under the following conditions: strain rate = 3.8 × 10⁻² s⁻¹; sample length between jaws = 50 ± 3 mm.

Self-Healing Tests. Self-healing behavior of dumbbell-shaped gel specimens was investigated by first cutting them at both gel zones locating 6 mm away from the interface region. For cylindrical gel specimens, they were cut in the middle into two equally sized pieces. The damaged gel samples were then self-healed by keeping the cut surfaces in contact for 1 h at 80 °C in a water vapor-saturated glass chamber. Thereafter, uniaxial compression and elongation tests were conducted as described above. The results were compared with those of the virgin gel samples.

RESULTS AND DISCUSSION

Preliminary experiments reveal two requirements for preparing mechanical strong hybrid hydrogels with smooth and robust interfaces (see Supporting Information): (i) Swelling ratios of the gel components of hybrids should not differ significantly from each other. Otherwise, the mismatch in the swelling ratios resulted in their rupture in aqueous environment (Figure S5). (ii) The interface region in hybrids should exhibit a smooth transition from one to another gel zone (Figure S6). Hybrid hydrogels composed of the following gel components satisfied these requirements (Scheme 1)—component 1 (C1): hydrogel derived from DMA/C18A monomer mixture at a molar ratio of 70/30; components 2 and 3 (C2, C3): hydrogels derived from DMA/C17.3M (C2) and DMA/C12M monomer mixtures (C3) at equimolar ratios.

Water contents as well as thermal and tensile mechanical properties of C1/C2 and C1/C3 hybrid hydrogels together with their components are compiled in Table 1. The gel fractions of all hydrogels were unity, indicating complete conversion of the monomers to the supramolecular network structure. The water content of the components of hybrids is between 10 and 27 wt % which decreases with increasing hydrophobic monomer content or with increasing side alkyl chain length. DSC measurements reveal that the C1 gel component consisting of DMA and C18A segments is a semicrystalline hydrogel with a melting temperature of 48 °C (Table 1). The C2 component composed of DMA and C17.3M segments has a lower melting temperature, 35 °C, due to the methyl group on the backbone of C17.3M units limiting the alignment of side alkyl chains.²⁶ In contrast, C3 component consisting of DMA and C12M segments is in amorphous state due to the shorter alkyl chain length of C12M units.^{35–37}

Figure 3a shows the image of a dumbbell-shaped C1/C2-hybrid gel specimen consisting of C2 (left) and C1 components

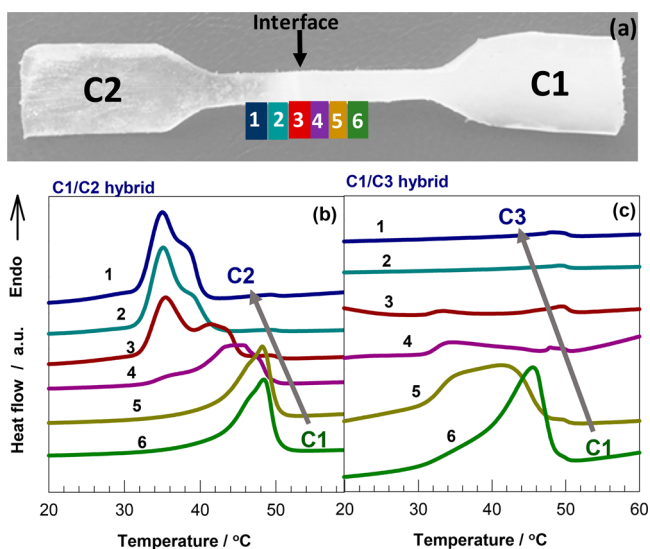


Figure 3. (a) Image of a C1/C2-hybrid gel specimen where the interface region is indicated by an arrow. (b, c) DSC scans conducted on C1/C2 (b) and C1/C3 hybrids (c) at six different locations in their interface region. The numbers correspond to the location numbers in the upper image.

(right). The figure also shows six different locations at the interface region between the C2 and C1 zones, labeled by 1 to

6, where DSC measurements were conducted. DSC scans of these locations are presented in Figure 3b, where the numbers on the curves are the location numbers in the upper image. T_m gradually decreases from 48 to 35 °C, i.e., from T_m of C1 to that of C2 as one moves from C1 to C2 zones along the interface region, indicating perfect fusion of the two gel components. Similar measurements were also conducted on C1/C3 hybrid gel specimens. Figure 3c shows that the melting peak appearing at 48 °C in C1 zone first broadens and then gradually disappears as the sample position approaches to the amorphous C3 zone of hybrid, indicating complete mixing of the gel components at the interface.

Uniaxial tensile tests were carried out on dumbbell-shaped hybrid hydrogels at 24 ± 1 °C. The ends of the gel specimens were clamped in metal grips while the interface region between their gel components was in the middle of the inner width of the specimens (Figures 4c,d). The solid curves in Figures 4a,b show tensile stress–strain curves of C1/C2 and C1/C3 hybrids, respectively, where the nominal stress σ_{nom} is plotted against the strain ϵ . The dashed curves in the figures are stress–strain curves of their gel components. The results reveal that the tensile mechanical properties of hybrids represent the average of those of their components. C1/C2 hybrid has a Young's modulus of 79 ± 9 MPa and tensile strength of 3.9 ± 0.2 MPa while C1/C3 hybrid exhibits a lower modulus and tensile strength (Table 1) but a higher stretch at break (457% vs 113%) due to the contribution of its highly stretchable C3 component. The important point is that the hybrid gel specimens subjected to tensile tests never break at their

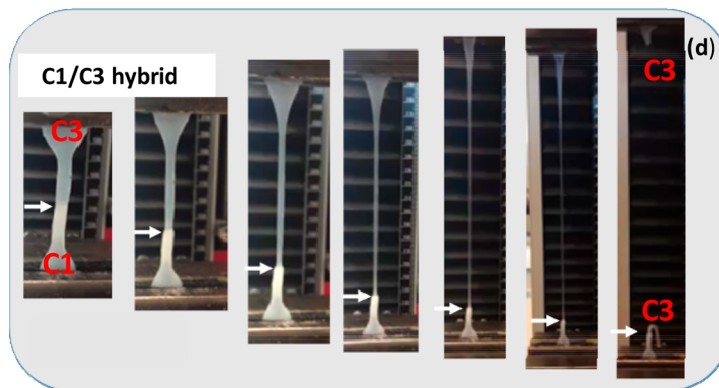
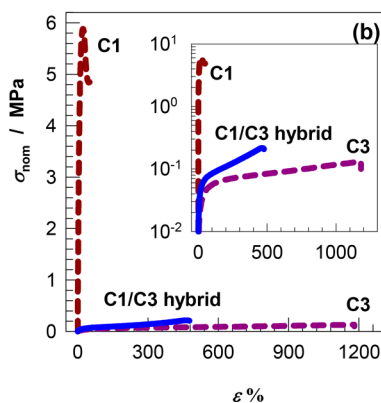
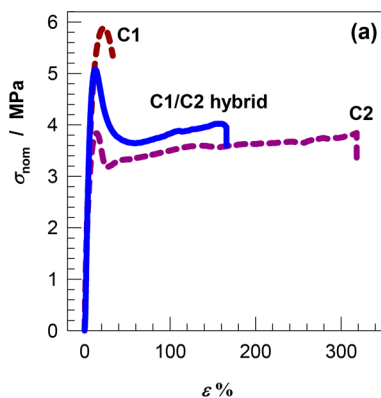


Figure 4. (a, b) Tensile stress–strain curves of C1/C2 and C1/C3 hybrids (solid curves) and their components (dashed curves) at 24 ± 1 °C. The inset to (b) shows semilogarithmic plots of the curves. (c, d) Images during the tensile tests of C1/C2 (c) and C1/C3 hybrid gel specimens. The interface regions are indicated by arrows.

interface regions as illustrated in Figures 4c,d. The interface regions indicated by white arrows remain intact under stress, and the fracture occurs at one of the gel zones of hybrid hydrogels.

The intactness of the interface region of hybrids at their fracture reveals higher mechanical strength of the interface as compared to one or both of the gel components. To demonstrate this feature, C1 + C2 and C1 + C3 mixture gels mimicking the interface regions were subjected to tensile tests. Figure 5a shows typical tensile stress–strain curves of C1 and

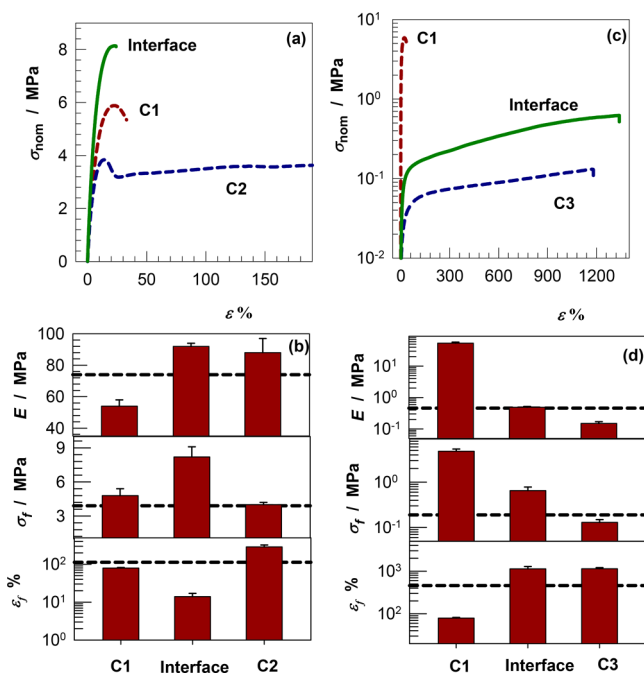


Figure 5. (a, c) Tensile stress–strain curves of the gel components and mixture gels representing the interface region of hybrids. Temperature = 24 ± 1 °C. (b, d) Young's modulus E , fracture stress σ_f , and strain ϵ_f of the gel components and the interface region of hybrids. The dashed lines represent the values for hybrid hydrogels.

C2 gel components and the C1 + C2 mixture gel, denoted as interface, while Figure 5b and Table 1 present their Young's modulus E , fracture stress σ_f , and strain ϵ_f . The dashed lines in Figure 5b indicate the values for hybrid hydrogels. The Young's modulus and tensile strength of C1/C2 interface are 92 ± 2 and 8.2 ± 0.9 MPa, respectively, which are much higher than those of the gel components. This is due to the higher degree of crystallinity of the mixture gel as compared to the gel components (16% vs 12%, Table 1) as well as due to the formation of more ordered crystalline domains in the presence of mixed hydrophobes leading to increased strength of hydrogels.²⁴ This explains why the interface of C1/C2 hybrid is stronger than both of its C1 and C2 gel zones. Several tests showed that C1/C2 hybrid always breaks at C2 region, as illustrated in Figure 4c, likely because C2 part yields and weakens before yielding of the C1 part (Table 1 and Figure 4a).

Figures 5c,d show tensile stress–strain curves and mechanical parameters of the interface of C1/C3 hybrid together with its C1 and C3 components. Both the modulus and strength of the interface are higher than the C3 gel component, suggesting that C3 zone of the hybrid would rupture under stress while the interface remains robust. The images shown in Figure 4d

indeed demonstrate that the rupture of the hybrid occurs at its C3 part.

Uniaxial compression tests were conducted on cylindrical gel specimens consisting of C2 or C3 core surrounded by the C1 outer layer. The solid and dashed curves in Figures 6a,b

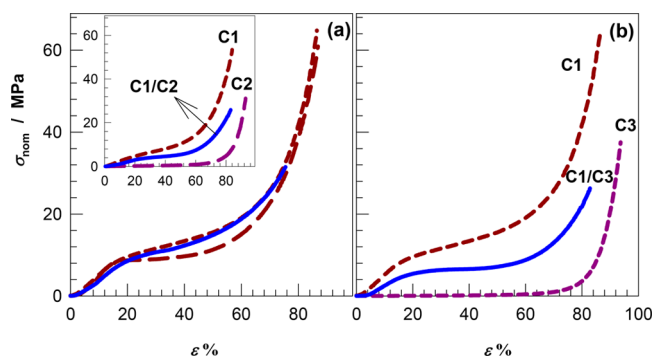


Figure 6. Compressive stress–strain curves of C1/C2 (a) and C1/C3 hybrids (b) and their components at 24 ± 1 °C shown by solid and dashed curves, respectively. The inset shows the data recorded at 37 °C.

represent compressive stress–strain curves of C1/C2 and C1/C3 hybrids and their gel components, respectively. The general trend is that the hybrids exhibit a lower compressive strength as compared to their gel components (Table S1). This is attributed to the easier appearance of microcracks in the hybrid due to the pressure of the hard shell on the soft core. The Young's modulus and compressive strength of C1/C2 hybrid are 47 ± 6 and 30 ± 4 MPa while those of C1/C3 are 32 ± 5 and 24 ± 3 , respectively, revealing that they both are good candidates to mimic the IVD. Figure 6a also shows that the initial mechanical properties of C1/C2 hybrid and its components are similar; i.e., their moduli are between 47 and 62 MPa. The inset to Figure 6a presents stress–strain curves of C1, C2, and C1/C2 gels measured at 37 °C which is between the melting temperatures of the C1 and C2 zones. Because the crystalline domains in C2 zone melts at 37 °C, as also seen from opaque-to-transparent transition in C2 zone (Scheme 1), the modulus of this zone decreases from 62 ± 7 to 0.34 ± 0.04 MPa, thus producing at the body temperature a hybrid hydrogel consisting of a soft core surrounded by a hard shell.

Presence of crystalline domains in both C1 and C2 zones of hybrid hydrogels resulted in drastic changes in their mechanical properties depending on the temperature. This feature is presented in Figure 7a where the storage moduli G' of C1/C2 and C1/C3 hybrids together with their gel components are plotted against temperature during heating from 5 to 80 °C at a heating rate of 5 °C min^{-1} . G' of the C1 component is 10 MPa at 5 °C, while it rapidly decreases at around its T_m , 48 °C, and finally becomes 0.06 MPa at 80 °C. More than 2 orders of magnitude decrease in the modulus of the C1 upon heating is totally reversible with a thermal hysteresis due to the lower recrystallization temperature (Table 1), as also reported before for semicrystalline hydrogels.^{25,29} A similar change in G' is observable for the C2 component except that the drastic decrease in G' occurs at its T_m of 35 °C. In contrast, G' of the C3 component only slightly decreases with temperature due to the absence of crystalline domains. The results also show that the modulus–temperature curves of hybrid hydrogels locate between those of their components, indicating that they both contribute to their overall viscoelastic response. Frequency-

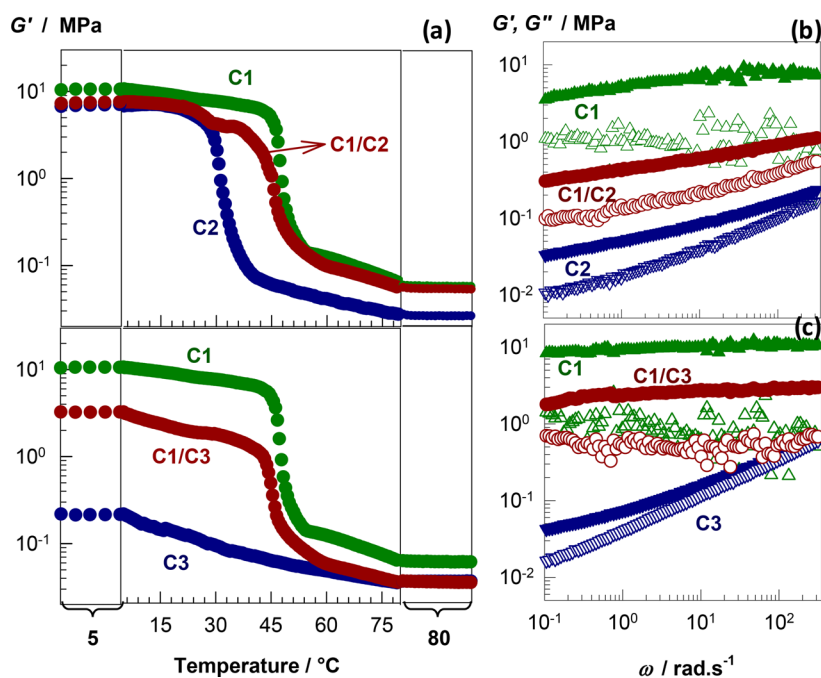


Figure 7. (a) Storage modulus G' of C1/C2 (upper panel) and C1/C3 hybrids (bottom panel) and their gel components during heating from 5 to 80 $^{\circ}\text{C}$ at a rate of 5 $^{\circ}\text{C min}^{-1}$, $\omega = 6.3 \text{ rad s}^{-1}$ and $\gamma_0 = 0.1\%$. (b, c) Frequency dependences of G' (filled symbols) and the loss modulus G'' (open symbols) of C1/C2 (b) and C1/C3 hybrids (c) and their components. Temperature = 37 (b) and 25 $^{\circ}\text{C}$ (c). $\gamma_0 = 0.1\%$.

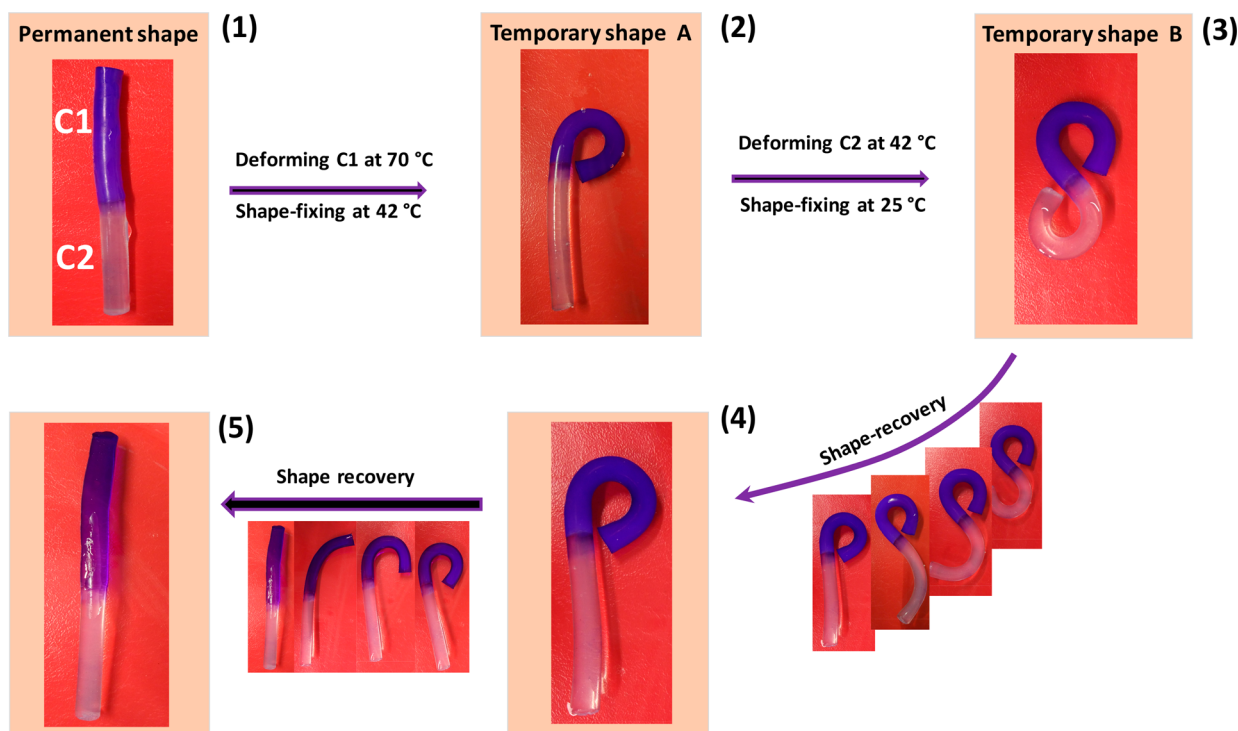


Figure 8. Images demonstrating pseudo triple-shape-memory behavior of C1/C2 hybrid hydrogels. Permanent shape (1), temporary shapes A and B (2, 3), and successive shape recoveries at 42 and 70 $^{\circ}\text{C}$ (4, 5).

sweep tests conducted on C1, C2, and C1/C2 gels at 25 $^{\circ}\text{C}$, i.e., below their T_m 's, show similar viscoelastic spectra (Figure S7). G' is independent of frequency, and it is much larger than the loss modulus G'' , as typical for strong gels. However, at 37 $^{\circ}\text{C}$, i.e., between the T_m 's of C1 and C2 gels, C1 gel is still a strong gel with a weak frequency dependence while C2 becomes a weak gel with a G'' approaching to G' at high

frequencies (Figure 7b). Similar viscoelastic spectra but at 25 $^{\circ}\text{C}$ were obtained on C1/C3 hybrids composed of semicrystalline C1 and amorphous C3 zones (Figure 7c).

Because the C1/C2 hybrid exhibits dual melting behavior with two separate T_m 's of 48 and 35 $^{\circ}\text{C}$ in its gel components, it is capable of memorizing two temporary shapes, known as the triple-shape-memory effect.³⁸ Figure 8 demonstrates triple-

shape-memory capability of a C1/C2 gel specimen. The image labeled by (1) is its permanent shape where the C1 zone is blue-violet colored with crystal violet for clarity. The gel is first heated to 70 °C (above both T_m 's), and its C1 zone is deformed. When the gel is cooled to 42 °C, i.e., between the two T_m 's of the gel zones, the temporary shape A is fixed due to the formation of crystalline domains in C1 zone (image 2). In the second step, the still melted C2 zone at 42 °C is deformed into the temporary shape B which is then fixed by cooling to 25 °C, i.e., below T_m of C2 zone (image 3). For the shape recovery, the gel is first heated to 42 °C to recover the temporary shape A while further heating to 70 °C recovers the permanent shape (images 4 and 5).

For the present supramolecular hydrogels, hydrophobic associations and crystalline domains act as netpoints and switching segments, respectively, responsible for the shape-memory effect. At temperatures above T_m , hydrophobic associations formed by melting of alkyl crystals determine the permanent shape of the hydrogel. In this state, the hydrogel can easily be deformed under loading to assign temporary shapes to its gel zones. Upon cooling below T_m , side alkyl chains forming crystalline domains fix the temporary shapes of the hydrogel. In typical triple-shape-memory hydrogels, there are two separated crystallizable hydrophobic domains (switching domains) with different T_m 's distributed homogeneously over the whole gel sample.³⁹ However, in the present hybrid hydrogel, the switching domains are localized in the gel zones, and thus, although each zone has dual shape-memory function, the whole hybrid exhibits triple-shape-memory effect, which may be termed as “pseudo triple-shape-memory” behavior. Shape-memory tests conducted on C1/C3 hybrids revealed existence of shape-memory function only at C1 zone while the C3 zone was unable to fix the temporary shape due to the absence of crystalline domains.

Because of the supramolecular nature, hybrid hydrogels have the ability to self-heal on both of their gel zones. Cyclic mechanical tests are a mean to detect the self-healing ability of cross-linked materials via monitoring the reversible nature of their cross-links. The cyclic tests were carried out by stretching C1/C2 gel specimens at a strain rate of $3.8 \times 10^{-2} \text{ s}^{-1}$ up to a maximum strain ϵ_{max} and then unloading at the same rate up to zero strain, followed by repeating these loading and unloading steps at the same strain rate. Figure 9a shows 20 successive tensile cycles composed of loading (upward curves) and unloading steps (downward curves) up to ϵ_{max} of 30%. It is seen that the neck region shown during the first loading step disappears in the following loadings, indicating a significant damage in the gel. Indeed, the hysteresis energy U_{hys} which is proportional to the number of bonds broken during a mechanical cycle is 0.92 MJ m^{-3} for the first cycle while it reduces to 0.45 MJ m^{-3} in the second cycle. U_{hys} further gradually decreases with increasing cycle number and becomes 0.24 MJ m^{-3} after 20th cycle, revealing that around 70% of intermolecular bonds in the gel specimen are broken. The damaged gel specimen was then taken out of the tensile tester and immersed in a water bath at 50 °C for 1 min followed by bringing to the test temperature of 24 °C. The sample was again subjected to 20 successive tensile cycles. This procedure was repeated twice, and the results are shown in Figures 9b,c. It is seen that heating the gel above T_m of the gel components and subsequent cooling to 24 °C recover the neck region so that similar hysteresis energies could be obtained. For instance, U_{hys} energies for the first cycles in Figures 9b and 9c are 0.86 and

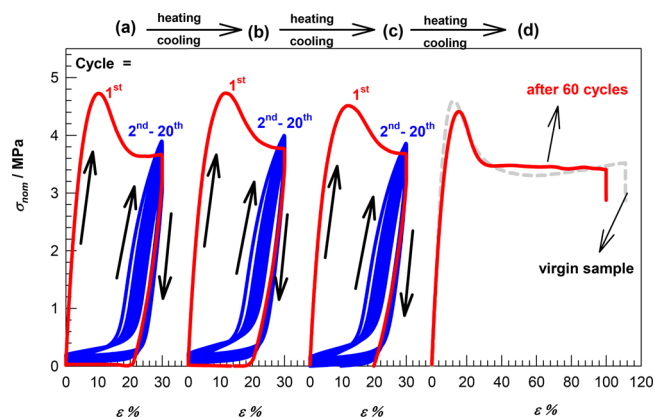


Figure 9. (a–c) Three sets of successive 20 tensile cycles separated by the thermal treatment for a C1/C2 gel specimen. $\epsilon_{\text{max}} = 30\%$. (d) Stress–strain curve of C1/C2 after subjecting 60 tensile cycles. For comparison, stress–strain curve of a C1/C2 gel sample is also shown by the dashed curve.

0.90 MJ m^{-3} , respectively, revealing that 93–98% bonds broken could be recovered by heating at 50 °C for 1 min. The damaged gel sample after subjecting to 60 tensile cycles was again repaired by the thermal treatment as described above and then stretched up to the fracture point. The solid and dashed curves in Figure 9d present stress–strain curves of the repaired sample and the virgin one, respectively. The repaired sample fractures at a stretch ratio of 97% under around 3.4 MPa stress, which are close to that of the virgin sample ($113 \pm 35\%$ at $3.9 \pm 0.2 \text{ MPa}$), revealing thermally induced self-healing ability of C1/C2 hybrid hydrogels.

To determine self-healing efficiency of hybrid hydrogels, dumbbell-shaped gel specimens were first cut at both gel zones locating 6 mm away from the interface region. This is illustrated in Figure 10a for a C1/C2 hybrid sample where white arrows indicate the cut regions while the yellow arrow shows the interface region. After bringing the cut surfaces together and keeping the sealed gel samples at 80 °C for 1 h followed by cooling to room temperature, they merged into a single piece. Figure 10 b shows typical tensile stress–strain curves of healed (dashed curve) and virgin C1/C2 and C1/C3 hybrid hydrogels (solid curves). Cutting at both gel zones of C1/C2 hybrid gel specimen followed by healing at 80 °C significantly reduces the ultimate mechanical properties, and the sample broke at the cut region before the yield point. However, when cut is created only at C2 zone, the healed sample again shows yielding behavior, and the healing efficiency with respect to fracture stress and strain becomes 73 ± 7 and $62 \pm 5\%$, respectively. Moreover, the fracture always occurred at C2 part of the hybrid but at a different location than the cut region. The C1/C3 hybrid exhibited above 80% healing efficiencies independent of the location of the cuts, and the fracture always occurred at the C3 region but at a different location. Compression tests were also conducted by cutting cylindrical hybrid gel specimens in the middle into two equally sized pieces and then bringing the cut surfaces together, as described above. As seen in Figure 10c, complete healing could be obtained on both C1/C2 and C1/C3 hydrogel hybrids.

Self-healing behavior of hybrid hydrogels induced by heating above T_m is attributed to the melting of crystalline domains at the cut region producing nonassociated alkyl side chains. Similar to the orientation of surfactant molecules at the water–air interface,⁴⁰ alkyl side chains at the cut region will orient

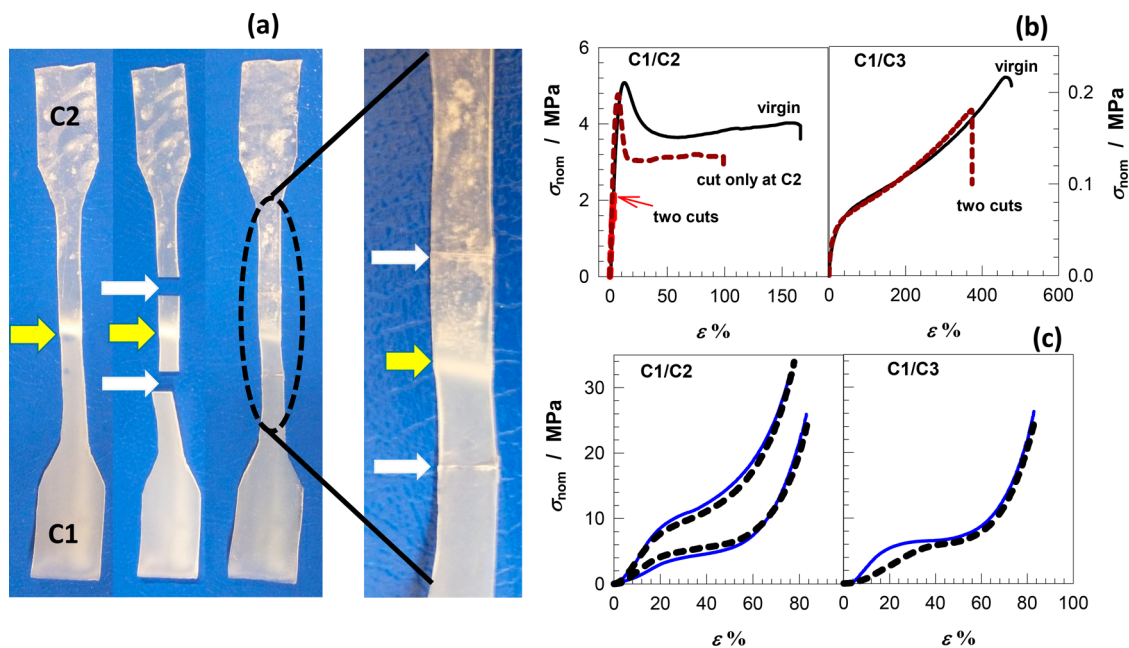


Figure 10. (a) Images of a C1/C2 gel specimen before and after cutting at both C1 and C2 zones and after repairing. Yellow arrow indicates the interface region while white arrows are the cut regions. (b, c) Stress–strain curves of virgin (solid curves) and healed C1/C2 and C1/C3 gel samples (dashed curves) obtained from tensile (b) and compression tests (c).

away from the bulk hydrogel phase containing 10–27 wt % water toward the cut surface which is in contact with air. After pressing the cut surfaces together above T_m and subsequent cooling below T_m , alkyl chains on both surfaces form crystalline domains and hydrophobic associations each other to decrease their exposure to the gel phase so that healing occurs with a high efficiency.

CONCLUSIONS

In contrast to high strength isotropic hydrogels reported so far, many biological systems are combinations of hard and soft materials integrated together through an extremely tough interface. We demonstrate that the polymerization of stratified monomer solutions of hydrophilic and hydrophobic monomers produces supramolecular hybrid hydrogels consisting of hard and soft components joined together through a strong interface. UV-initiated bulk copolymerization of stratified solutions containing the hydrophilic monomer DMA and the hydrophobic monomers C18A, C17.3M, or C12M carrying alkyl side chains of different lengths leads to the formation of supramolecular, semicrystalline hybrid hydrogels with tunable mechanical and thermal properties. By adjusting the copolymer composition, we were able to create gel/gel interfaces in hybrids that are stronger than their gel components so that they never rupture at the interface region. The hybrids exhibit a high modulus (0.46–74 MPa) and tensile strength (0.19–3.9 MPa) and sustain 24–30 MPa stresses at 78–83% compressions, which are comparable to the natural IVD. The hybrids have the ability to self-heal upon heating above T_m once one or both of their gel components are damaged. They also exhibit a pseudo triple-shape-memory effect arising from two melting temperatures belonging to the gel components of hybrids. The synthetic strategy presented here thus enables combination of multiple gel components in a single material leading to the preparation of multishape-memory hydrogels with multi-responsivity.

ASSOCIATED CONTENT

Supporting Information

The Supporting Information is available free of charge on the ACS Publications website at DOI: 10.1021/acs.macromol.8b00233.

Experimental details including sample preparation and characterization (PDF)

AUTHOR INFORMATION

Corresponding Author

*(O.O.) E-mail: okayo@itu.edu.tr.

ORCID

Oguz Okay: 0000-0003-2717-4150

Notes

The authors declare no competing financial interest.

ACKNOWLEDGMENTS

Work was supported by the Scientific and Technical Research Council of Turkey (TUBITAK), KBAG 114Z312. O.O. thanks the Turkish Academy of Sciences (TUBA) for the partial support.

REFERENCES

- Calvert, P. Hydrogels for soft machines. *Adv. Mater.* **2009**, *21*, 743–756.
- Seiffert, S., Ed.; *Supramolecular Polymer Networks and Gels*; Book Series Adv. Polym. Sci.; Springer: Berlin, 2015.
- Amaral, A. J. R.; Pasparakis, G. Stimuli responsive self-healing polymers: gels, elastomers and membranes. *Polym. Chem.* **2017**, *8*, 6464–6484.
- Creton, C. 50th Anniversary perspective: Networks and gels: Soft but dynamic and tough. *Macromolecules* **2017**, *50*, 8297–8316.
- Apostolakis, J.; Durant, T. J. S.; Dwyer, C. R.; Russell, R. P.; Weinreb, J. H.; Alae, F.; Beitzel, K.; McCarthy, M. B.; Cote, M. P.; Mazzocca, A. D. The enthesis: a review of the tendon-to-bone insertion. *Muscles Ligaments Tendons J.* **2014**, *4*, 333–342.

- (6) Rossetti, L.; Kuntz, L. A.; Kunold, E.; Schock, J.; Müller, K. W.; Grabmayr, H.; Stolberg-Stolberg, J.; Pfeiffer, F.; Sieber, S. A.; Burgkart, R.; Bausch, A. R. The microstructure and micromechanics of the tendon–bone insertion. *Nat. Mater.* **2017**, *16*, 664–670.
- (7) Nerurkar, N. L.; Elliott, D. M.; Mauck, R. L. Mechanical design criteria for intervertebral disc tissue engineering. *J. Biomech.* **2010**, *43*, 1017–1030.
- (8) Whatley, B. R.; Wen, X. Intervertebral disc (IVD): Structure, degeneration, repair and regeneration. *Mater. Sci. Eng., C* **2012**, *32*, 61–77.
- (9) Iatridis, J. C.; Nicoll, S. B.; Michalek, A. J.; Walter, B. A.; Gupta, M. S. Role of biomechanics in intervertebral disc degeneration and regenerative therapies: what needs repairing in the disc and what are promising biomaterials for its repair? *Spine J.* **2013**, *13*, 243–264.
- (10) Hu, Z.; Zhang, X.; Li, Y. Synthesis and application of modulated polymer gels. *Science* **1995**, *269*, 525–527.
- (11) Banik, S. J.; Fernandes, N. J.; Thomas, P. C.; Raghavan, S. R. A new approach for creating polymer hydrogels with regions of distinct chemical, mechanical, and optical properties. *Macromolecules* **2012**, *45*, 5712–5717.
- (12) Gargava, A.; Arya, C.; Raghavan, S. R. Smart hydrogel-based valves inspired by the stomata in plants. *ACS Appl. Mater. Interfaces* **2016**, *8*, 18430–18438.
- (13) Rose, S.; PrevotEAU, A.; Elzière, P.; Hourdet, D.; Marcellan, A.; Leibler, L. Nanoparticle solutions as adhesives for gels and biological tissues. *Nature* **2014**, *505*, 382–385.
- (14) Meddahi-Pellé, A.; Legrand, A.; Marcellan, A.; Louedec, L.; Letourneur, D.; Leibler, L. Organ repair, hemostasis, and in vivo bonding of medical devices by aqueous solutions of nanoparticles. *Angew. Chem., Int. Ed.* **2014**, *53*, 6369–6373.
- (15) Wirthl, D.; Pichler, R.; Drack, M.; Kettlguber, G.; Moser, R.; Gerstmayr, R.; Hartmann, F.; Bradt, E.; Kaltseis, R.; Siket, C. M.; Schausberger, S. E.; Hild, S.; Bauer, S.; Kaltenbrunner, M. Instant tough bonding of hydrogels for soft machines and electronics. *Sci. Adv.* **2017**, *3*, e1700053.
- (16) Yong, X.; Simakova, A.; Averick, S.; Gutierrez, J.; Kuksenok, O.; Balazs, A. C.; Matyjaszewski, K. Stackable, covalently fused gels: Repair and composite formation. *Macromolecules* **2015**, *48*, 1169–1178.
- (17) Beziau, A.; de Menezes, R. N. L.; Biswas, S.; Singh, A.; Cuthbert, J.; Balazs, A. C.; Kowalewski, T.; Matyjaszewski, K. Combining ATRP and FRP gels: Soft gluing of polymeric materials for the fabrication of stackable gels. *Polymers* **2017**, *9*, 186.
- (18) Deng, G.; Ma, Q.; Yu, H.; Zhang, Y.; Yan, Z.; Liu, F.; Liu, C.; Jiang, H.; Chen, Y. Macroscopic organohydrogel hybrid from rapid adhesion between dynamic covalent hydrogel and organogel. *ACS Macro Lett.* **2015**, *4*, 467–471.
- (19) Yuk, H.; Zhang, T.; Lin, S.; Parada, G. A.; Zhao, X. Tough bonding of hydrogels to diverse non-porous surfaces. *Nat. Mater.* **2016**, *15*, 190–196.
- (20) Meakin, J. R.; Reid, J. E.; Hukins, D. W. L. Replacing the nucleus pulposus of the intervertebral disc. *Clin. Biomech.* **2001**, *16*, 560–565.
- (21) Gloria, A.; Causa, F.; De Santis, R.; Netti, P. A.; Ambrosio, L. Dynamic-mechanical properties of a novel composite intervertebral disc prosthesis. *J. Mater. Sci.: Mater. Med.* **2007**, *18*, 2159–2165.
- (22) Wang, B. H.; Campbell, G. Formulations of polyvinyl alcohol cryogel that mimic the biomechanical properties of soft tissues in the natural lumbar intervertebral disc. *Spine* **2009**, *34*, 2745–2753.
- (23) Okay, O. Self-healing hydrogels formed via hydrophobic interactions. *Adv. Polym. Sci.* **2015**, *268*, 101–142.
- (24) Bilici, C.; Ide, S.; Okay, O. Yielding behavior of tough semicrystalline hydrogels. *Macromolecules* **2017**, *50*, 3647–3654.
- (25) Bilici, C.; Can, V.; Nöchel, U.; Behl, M.; Lendlein, A.; Okay, O. Melt-processable shape-memory hydrogels with self-healing ability of high mechanical strength. *Macromolecules* **2016**, *49*, 7442–7449.
- (26) Kurt, B.; Gulyuz, U.; Demir, D. D.; Okay, O. High-strength semi-crystalline hydrogels with self-healing and shape memory functions. *Eur. Polym. J.* **2016**, *81*, 12–23.
- (27) Uemura, Y.; McNulty, J.; Macdonald, P. M. Associative behavior and diffusion coefficients of hydrophobically modified poly-(N,N-dimethylacrylamides). *Macromolecules* **1995**, *28*, 4150–4158.
- (28) Relogio, P.; Martinho, J. M. G.; Farinha, J. P. S. Effect of surfactant on the intra- and intermolecular association of hydrophobically modified poly(N,N-dimethylacrylamide). *Macromolecules* **2005**, *38*, 10799–10811.
- (29) Bilici, C.; Okay, O. Shape memory hydrogels via micellar copolymerization of acrylic acid and n-octadecyl acrylate in aqueous media. *Macromolecules* **2013**, *46*, 3125–3131.
- (30) Mogri, Z.; Paul, D. R. Gas sorption and transport in side-chain crystalline and molten poly(octadecylacrylate). *Polymer* **2001**, *42*, 2531–2542.
- (31) Bisht, H. S.; Pande, P. P.; Chatterjee, A. K. Docosyl acrylate modified polyacrylic acid: synthesis and crystallinity. *Eur. Polym. J.* **2002**, *38*, 2355–2358.
- (32) Broadhurst, M. G. An analysis of the solid phase behavior of the normal paraffins. *J. Res. Natl. Bur. Stand., Sect. A* **1962**, *66A*, 241–249.
- (33) Jordan, E. F.; Feldeisen, D. W.; Wrigley, A. N. Side-chain crystallinity. I. Heats of fusion and melting transitions on selected homopolymers having long side chains. *J. Polym. Sci., Part A-1: Polym. Chem.* **1971**, *9*, 1835–1851.
- (34) Argun, A.; Can, V.; Altun, U.; Okay, O. Non-ionic double and triple network hydrogels of high mechanical strength. *Macromolecules* **2014**, *47*, 6430–6440.
- (35) Hempel, E.; Budde, H.; Höring, S.; Beiner, M. On the crystallization behavior of frustrated alkyl groups in poly(n-octadecyl methacrylate). *J. Non-Cryst. Solids* **2006**, *352*, 5013–5020.
- (36) Hiller, S.; Pascui, O.; Budde, H.; Kabisch, O.; Reichert, D.; Beiner, M. Nanophase separation in side chain polymers: new evidence from structure and dynamics. *New J. Phys.* **2004**, *6*, 10.
- (37) Tuncaboylu, D. C.; Argun, A.; Sahin, M.; Sari, M.; Okay, O. Structure optimization of self-healing hydrogels formed via hydrophobic interactions. *Polymer* **2012**, *53*, 5513–5522.
- (38) Bellin, I.; Kelch, S.; Langer, R.; Lendlein, A. Polymeric triple-shape materials. *Proc. Natl. Acad. Sci. U. S. A.* **2006**, *103*, 18043–18047.
- (39) Nöchel, U.; Behl, M.; Balk, M.; Lendlein, A. Thermally-induced triple-shape hydrogels: Soft materials enabling complex movements. *ACS Appl. Mater. Interfaces* **2016**, *8*, 28068–28076.
- (40) Berg, J. C. *An Introduction to Interfaces & Colloids: The Bridge to Nanoscience*; World Scientific: Singapore, 2010.